

High-Gain Step-Profiled Integrated Diagonal Horn-Antennas

George V. Eleftheriades and Gabriel M. Rebeiz, *Member, IEEE*

Abstract—Dipole excited integrated horn antennas are well established by now. Their main limitation stems from their large flare angle of 70° which is inherent in the anisotropic etching process of $\langle 100 \rangle$ silicon wafers. The large flare-angle does not allow for integrated horns with gains higher than 13 dB and for 10-dB beamwidths less than 90° . In this paper, a new step-profiled horn is proposed which reduces the effective flare angle of the horn and allows for gains in the region of 17 dB to 20 dB to be achieved. The symmetry of the horn's radiation pattern is enhanced by positioning the exciting dipole along the diagonal of the horn cavity. A specific design example is shown with a gain of 18.4 dB and a 10-dB beamwidth of 37° in the E , H and 45° planes. The coupling efficiency of this horn to a Gaussian beam is calculated to be 83%. An equivalent smooth envelope-horn (see text) was built at 12.1 GHz and the measured patterns agree well with theory. The integrated step-profiled horn is well suited for millimeter wave and Terahertz focal plane imaging arrays requiring a large number of elements.

I. INTRODUCTION

DIPOLE excited integrated horn antennas are well investigated in [1]–[4]. They consist of a strip-dipole antenna suspended on a thin dielectric membrane inside a pyramidal cavity etched in silicon. The antennas are free from surface-wave losses and fully integrated. However, the anisotropic etching of silicon used in their fabrication defines their flare angle to be 70° . The phase error introduced by the large flare angle limits the horn aperture size to less than 1.5λ -square resulting in a maximum gain of 13 dB. A step-profiled horn is proposed which improves the gain and the axial-symmetry of the radiation pattern (Fig. 1). As shown in figure 1, deliberate step-discontinuities are introduced between successive wafers resulting in a step-profiled horn with an effective flare-angle around 30° . A spherical wavefront emanating from the apex of the horn suffers a reduction of its surface each time it crosses a wafer discontinuity. In this way the wavefront reaches the aperture of the horn with a phase error which corresponds more closely to the smaller effective flare angle of the envelope-horn rather than to the 70° flare angle of each individual wafer. Furthermore, the exciting-strip dipole is placed diagonally inside the horn

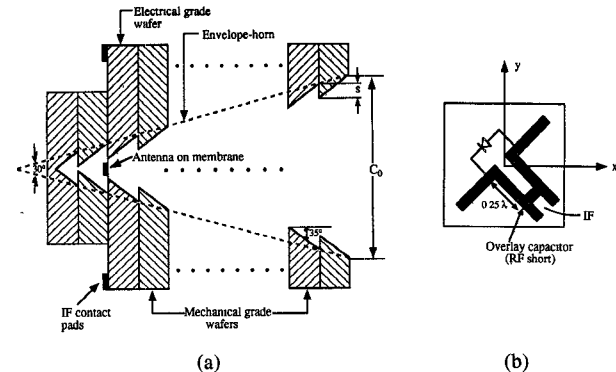


Fig. 1. (a) The step-profiled horn geometry. (b) Excitation membrane inside the horn.

to result in an enhancement of the circular-symmetry of the patterns and a reduction of the side-lobe level in the principal planes [5], [6].

The step-profiled horn is simple to build using integrated circuit techniques. The inside surface of the horn is evaporated with gold and therefore the walls of the horn are considered perfectly conducting. The reader is referred to [1], [4] for a detailed description of the fabrication process. The horn consists of an electronic-grade wafer and a number of mechanical-grade wafers. The dielectric-membrane, antennas, detectors, I.F. networks and electronics are all integrated on the electronic-grade wafer. The mechanical-grade wafers are just etched, aligned and glued together to form the required step-profile. As will be seen later the thickness of the mechanical-grade wafers is around 0.3λ which results in $450\ \mu\text{m}$ and $200\ \mu\text{m}$ thick wafers at 200 GHz and 450 GHz, respectively. This stepped-horn configuration can also be extended to two-dimensional imaging arrays with no additional machining, fabrication or alignment. The two-dimensional array offers plenty of space for the receiver electronics since the horn aperture is typically 3λ -square and the membrane is about 0.6λ -square. The antennas therefore occupy 4% of the electronic wafer space and 96% is available for the receiver electronics.

II. THEORETICAL ANALYSIS

A full-wave analysis has been performed on the step-profiled horn similar to the one performed for the analysis of a smooth strip-excited horn [2]. The geometry of the horn is approximated by a multisteped waveguide dis-

Manuscript received April 29, 1991; revised January 9, 1992. This work was supported by the NASA/Center for Space Terahertz Technology at the University of Michigan.

The authors are with the NASA/Center for Space Terahertz Technology, Electrical Engineering and Computer Science Department, University of Michigan, Ann Arbor, MI 48109-2122.

IEEE Log Number 9106968.

continuity and the corresponding generalized scattering matrices are directly combined together to generate the total scattering matrices of the structure. The horn is assumed to be mounted on an infinite ground plane and the transition to the half space is rigorously taken into consideration. Far-field patterns are calculated from the Fourier transform of the aperture field. Both TE and TM modes have been included in the analysis and modes up to the TE₇₆ and TM₇₆ have been retained in the numerical computations (for more details see [2]).

The strip-dipole excites the horn along its diagonal resulting in an equal tapering for the E and H aperture fields and leading to very similar E and H far-field patterns [5]. The diagonal horn however is circularly symmetric only under the paraxial approximation, that is, for narrow main beams. Otherwise the H -plane pattern is lower than the E -plane pattern by a factor of $\cos^2(\theta)$. This can be demonstrated by a simple TE₁₀/TE₀₁ modal analysis (with no phase error). Specifically, a diagonal horn with a square aperture of side C_o results in a far-field electric field given by (Fig. 1(b)):

E -plane field ($\phi = 45^\circ$):

$$\begin{aligned} E_\theta &= E(u) \\ E_\phi &= 0 \end{aligned} \quad (1)$$

H -plane field ($\phi = 135^\circ$):

$$\begin{aligned} E_\theta &= 0 \\ E_\phi &= E(u) \cos(\theta) \end{aligned} \quad (2)$$

where

$$E(u) = \frac{2\sqrt{2}C_o^2}{\pi} \left[\frac{\sin(u/\sqrt{2})}{u/\sqrt{2}} \right] \left[\frac{\cos(u/\sqrt{2})}{1 - 2u^2/\pi} \right] \quad (3)$$

and

$$u = \frac{kC_o}{2} \sin(\theta). \quad (4)$$

For horns without excessive phase error the same behavior is also verified by using the full-wave analysis instead of the simple TE₁₀/TE₀₁ modal analysis. A diagonal feeding dipole will therefore enhance the pattern symmetry of horns with moderate flare-angle and large apertures but it will fail for horns with small apertures. For this reason the diagonal dipole is well-suited for the step-profiled approach which allows for small effective flare angles and large apertures.

III. COUPLING TO A GAUSSIAN BEAM

The coupling of the horn antennas to a Gaussian beam has been calculated by expanding the aperture field into Hermite-Gaussian modes [8], [9]. Since it is assumed that the horn is mounted on a ground plane, the tangential aperture field is of the form:

$$\bar{E}_{ap}(x, y) = \begin{cases} \bar{E}_{ap}(x, y), & \text{on aperture} \\ 0, & \text{otherwise.} \end{cases} \quad (5)$$

The copolarized component of the aperture field (the one that is parallel to the direction of the exciting strip-dipole) can be expanded into a set of orthogonal Hermite-Gaussian modes:

$$\mathcal{E}_{ap,co}(x, y) = \sum_{m=0}^{\infty} \sum_{n=0}^{\infty} d_{mn} G_{mn}(x, y). \quad (6)$$

In (6) above, the Gaussian modes G_{mn} on the aperture of the horn can be expressed in the form [11]:

$$\begin{aligned} G_{mn}(x, y) &= \frac{w_o}{w_{ap}} e^{(-jkz_{ap})} \exp \left[\left(-\frac{jk(x^2 + y^2)}{2R_{ap}} \right) \right] \\ &\cdot \exp \left[\left(j(m + n + 1) \arctan \left(\frac{\lambda z_{ap}}{\pi w_o^2} \right) \right) \right] \\ &\cdot \exp \left[\left(-\frac{x^2 + y^2}{w_{ap}^2} \right) \right] H_m \left(\frac{\sqrt{2}x}{w_{ap}} \right) H_n \left(\frac{\sqrt{2}y}{w_{ap}} \right) \end{aligned} \quad (7)$$

where H_m is the Hermite polynomial of order m , w_o is the beam waist half width and z_{ap} is the distance from the beam waist to the aperture of the horn (Fig. 2). The beam radius of curvature at the aperture of the horn is given by $R_{ap} = z_{ap}[1 + (\pi w_o^2/\lambda z_{ap})^2]$ and the beam half width at the aperture by $w_{ap} = w_o[1 + (\lambda z_{ap}/\pi w_o^2)^2]^{1/2}$. In order to facilitate the notation, we define the inner product between two functions $\bar{a}(x, y)$ and $\bar{b}(x, y)$ on the aperture plane to be

$$\langle \bar{a}, \bar{b} \rangle = \int_{-\infty}^{\infty} \int_{-\infty}^{\infty} \bar{a}^* \cdot \bar{b} dx dy. \quad (8)$$

The dot product in (8) should be replaced by ordinary multiplication when the arguments of the inner product, \bar{a} and \bar{b} are scalar quantities. With this definition of an inner product, the Gaussian modes G_{mn} satisfy the orthogonality relation [13]:

$$\langle G_{mn}, G_{pq} \rangle = \frac{\pi w_o^2}{2} 2^{m+n} m! n! \delta_{mp} \delta_{nq} \quad (9)$$

where δ is the Kronecker symbol.

Also it is assumed that the electric and magnetic fields on the aperture of the horn are related by

$$\bar{H}_{ap} = \frac{\hat{z} \times \bar{E}_{ap}}{Z_o} \quad (10)$$

where Z_o is the free-space intrinsic impedance. This assumption is valid for electrically large apertures with moderate phase error. Under the above assumption the fractional power carried by the (mn^{th}) Gaussian mode is given by

$$\eta_{mn} = \frac{|d_{mn}|^2 \langle G_{mn}, G_{mn} \rangle / 2Z_o}{\langle \bar{E}_{ap}, \bar{E}_{ap} \rangle / 2Z_o}. \quad (11)$$

Using the orthogonality of the Gaussian modes as expressed in (9) to evaluate the modal coefficients d_{mn} of

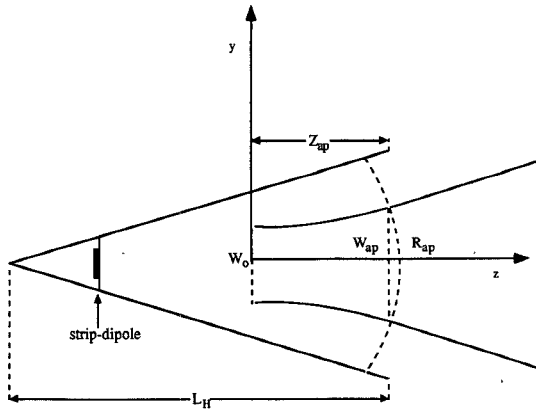


Fig. 2. The coupling of a Gaussian beam to a horn-antenna.

equation (6) yields

$$\eta_{mn} = \frac{|\langle G_{mn}, \mathcal{E}_{ap,co} \rangle|^2}{\langle G_{mn}, G_{mn} \rangle \langle \bar{\mathcal{E}}_{ap}, \bar{\mathcal{E}}_{ap} \rangle}. \quad (12)$$

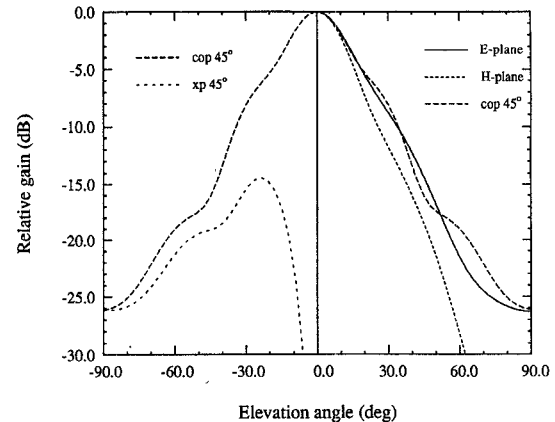
The above expression for the coupling efficiency complies with the expression derived in [7] using far-field analysis. For the fundamental Gaussian mode G_{oo} , (12) readily gives

$$\eta_{00} = \frac{\left| \iint_{\text{aperture}} e^{jk(x^2 + y^2)/2R_{ap}} e^{-(x^2 + y^2)/w_{ap}^2} E_{ap,co}(x, y) dx dy \right|^2}{\frac{\pi w_{ap}^2}{2} \iint_{\text{aperture}} |\bar{E}_{ap}(x, y)|^2 dx dy} \quad (13)$$

In (13) the aperture beam half-width w_{ap} is chosen so that the coupling η_{00} is maximized [8]. The aperture field $E_{ap,co}$ has been obtained from the full-wave analysis. Also the beam radius of curvature on the aperture R_{ap} has been assumed equal to the smooth envelope-horn axial length L_H (Fig. 2). This assumption was verified by calculating the phase error of the aperture field and by then determining the corresponding wavefront radius of curvature at the aperture of the horn.

IV. DESIGN EXAMPLE AND MEASUREMENTS

As was mentioned in the introduction, the 70° -flare angle of the smooth integrated horns does not allow for large apertures and high gains. This can be seen by considering a 70° -flare diagonal horn of 2.92λ -square aperture attempted designed for a gain around 18-dB. It is apparent from Fig. 3 that the excessive phase error does not allow either for high aperture efficiency (31%, 15 dB gain) or for satisfactory circular symmetry. This problem has been attacked by designing a step-profiled diagonal horn with a lower effective flare angle. A 18-dB step-profiled horn has been designed using 12 and 16 70° -flare wafers in an effort to approximate the radiation characteristics of their

Fig. 3. A 70° smooth diagonal horn with a 2.92λ -square aperture. The exciting strip dipole is at 0.39λ from the apex.

30° flare-angle diagonal smooth-walled envelope-horn (Fig. 1). The corresponding wafer thicknesses are 0.4λ and 0.31λ , respectively.

The results of the computer simulations for the patterns of the 12 and 16 steps horns are shown in Figs. 4 and 5, respectively. Also, the comparison of the step-profiled patterns with their smooth-walled envelope-horn in the E and 45° planes is shown in Fig. 6. The copolarized and cross-polarized patterns in the 45° -plane were calculated according to Ludwig's 3rd definition [10]. The radiation characteristics of the profiled horns are compared with those of the 30° envelope-horn in Table I.

From this comparison it is obvious that the 16-wafer horn performs almost like its smooth envelope-horn counterpart. The 12-wafer on the other hand is not as efficient. This is because the 12-wafer horn involves relatively large step discontinuities ($S = 0.173\lambda$, see Fig. 1) as opposed to the corresponding $S = 0.134\lambda$ for the 16-wafer horn. Our calculations indicate that for achieving a good approximation to the radiation characteristics of the smooth-walled envelope-horn, the step discontinuities of the profiled horn should not exceed 0.15λ . Larger step discontinuities result in additional phase error effects, higher cross-polarization and a corresponding reduction of both the antenna aperture efficiency and its coupling to a Gaussian beam. It is also observed from Figs. 4–6 that the 45° -plane pattern develops a characteristic shoulder for both the profiled and the smooth-walled 30° -flare horn. The reason for this broadening is that for diagonal horns of moderate flare angle (which mainly excite the TE_{10}/TE_{01} modes), the aperture field on the intercardinal planes is not well tapered and does not vanish at the edges of the aperture. The consequence of this non-tapered phase error on the intercardinal planes is that the 45° patterns develop the observed shoulders. It should be noted here that in the case of the wide flare-angle horn of Fig. 3, higher order modes taper the aperture field in the intercardinal planes and therefore the 45° -pattern does not have very distinct shoulders.

Since a step-profiled horn with a step-discontinuity not exceeding 0.15λ has compared well to its envelope-horn,

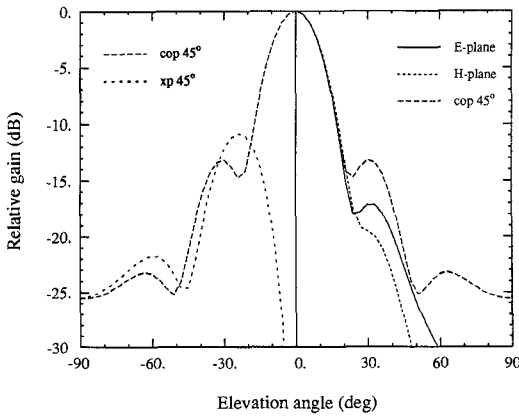


Fig. 4. Patterns for the diagonal 12-wafer, 2.92λ -square aperture horn. The thickness of each wafer is 0.4λ . The exciting strip dipole is at 0.7λ from the apex.

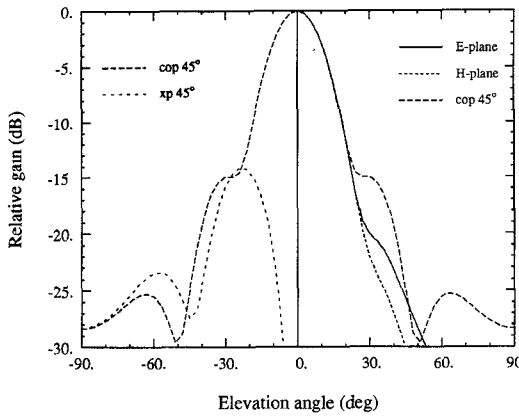


Fig. 5. Patterns for the diagonal 16-wafer 2.92λ -square aperture horn. The thickness of each wafer is 0.31λ . The exciting strip dipole is at 0.62λ from the apex.

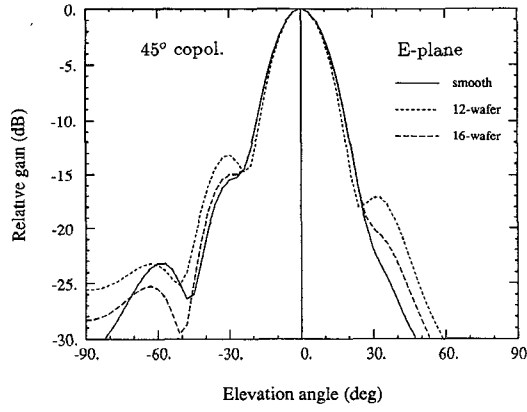


Fig. 6. Comparison of the 45° copol. (left) and E -plane patterns (right) between the 12-wafer horn, the 16-wafer horn and their smooth 30° flare-angle envelope-horn.

a 12.1 GHz dipole-fed microwave model for the smooth-walled envelope-horn was built, measured and compared to theory. The model has a 30° flare angle, a 2.92λ -square aperture and it is diagonally fed with a 0.4λ strip dipole placed 1.12λ away from the apex. As it can be observed (Figs. 7 and 8), the experimental patterns agree very well

TABLE I
RADIATION CHARACTERISTICS OF DIAGONAL 2.92λ -SQUARE APERTURE HORNS

Antenna Type	12-Wafer	16-Wafer	30° -Smooth
Gain	17.9 dB	18.4 dB	18.6 dB
Aperture effic.	58%	64%	67%
10 dB beamwidth	35°	37°	37°
Gaussian coupl.	68%	83%	85%
Cross-pol (45°)	-11.5 dB	-14 dB	-16.5 dB

The wafer thickness is 0.4λ for the 12-wafer and 0.31λ for the 16-wafer horn.

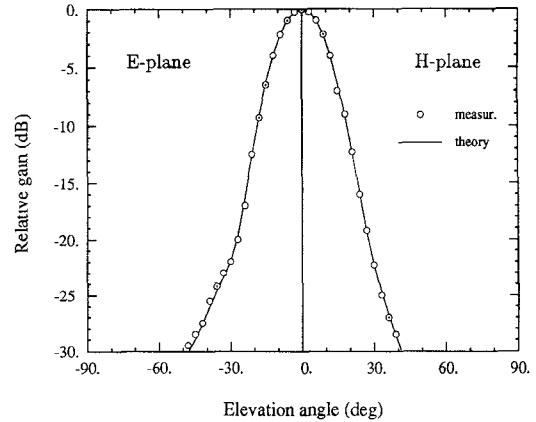


Fig. 7. Comparison between measurements done at 12.1 GHz and theory for the E -plane (left) and H -plane (right) patterns of the 30° flare-angle smooth envelope-horn.

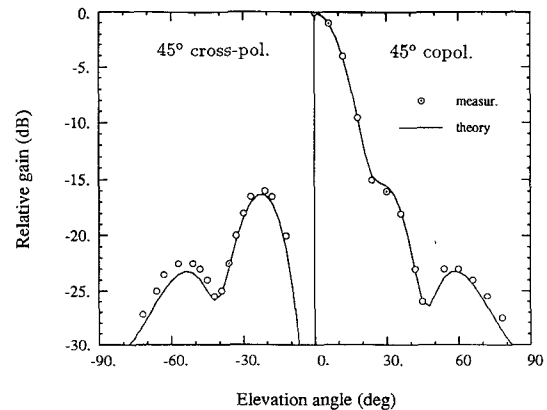


Fig. 8. Comparison between measurements done at 12.1 GHz and theory for the $\pm 45^\circ$ cross-pol (left) and copol. (right) patterns of the 30° flare-angle smooth envelope-horn.

with the theory. The measured resonant dipole input impedance at 8 GHz is shown in Fig. 9. It is around 220Ω and it has approximately a 5% bandwidth.

V. PRACTICAL RECOMMENDATIONS

For any practical realization of a step-profiled horn the step-size should be kept below 0.15λ . In this case the effect of the step-discontinuities is insignificant and therefore only the equivalent smooth envelope horn should be considered. Furthermore, we have verified that for di-

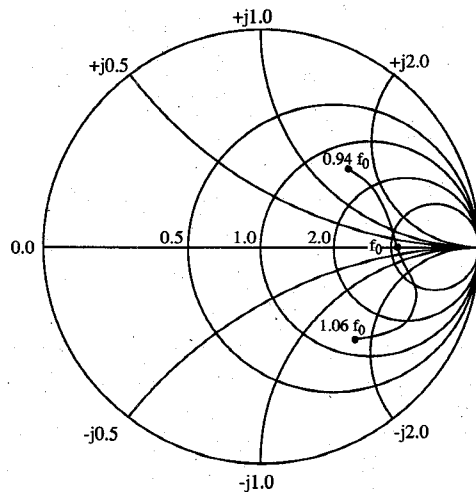


Fig. 9. Measured dipole input impedance versus frequency for a 0.4λ strip-dipole of width 0.05λ positioned 1.12λ away from the apex of the 30° flare-angle smooth envelope-horn. The measured resonant resistance at $f_0 = 8$ GHz is 220Ω .

poles located deep inside the horn, the patterns of the dipole-fed horn are identical to the patterns of the corresponding waveguide-fed horn. Consequently simple dominant-mode theory for waveguide-fed diagonal horns can be employed for the design of practical integrated step-profiled horns [5], [6], [12].

VI. CONCLUSION

A new step-profiled integrated-horn antenna is proposed. The antenna allows for gains in the range of 17 dB–20 dB to be achieved using standard $\langle 100 \rangle$ silicon wafers. The antenna is diagonally-fed and exhibits very good circular symmetry within the 10-dB beamwidth. It has a fundamental Gaussian coupling efficiency of 83%. We have demonstrated that the profiled antenna has a radiation pattern similar to that of its smooth envelope-horn, provided that the wafer discontinuity between successive wafers does not exceed 0.15λ . The integrated stepped-profiled horn performs much better than a corresponding smooth 70° flare-angle integrated horn of the same aperture size. The integrated step-profiled horn is very well-suited for radio-astronomical and remote-sensing millimeter-wave imaging arrays requiring a large number of focal-plane elements.

ACKNOWLEDGMENT

The authors would like to thank Dr. J. F. Johansson of Chalmers University, Sweden, for useful discussions.

REFERENCES

- [1] G. M. Rebeiz, D. P. Kasilingam, P. A. Stimson, Y. Guo, and D. B. Rutledge, "Monolithic millimeter-wave two-dimensional horn imaging arrays," *IEEE Trans. Antennas Propagat.*, vol. 28, pp. 1473–1482, Sept. 1990.
- [2] G. V. Eleftheriades, W. Y. Ali-Ahmad, L. P. B. Katehi, and G. M. Rebeiz, "Millimeter-wave integrated-horn antennas Part I: Theory, Part II: Experiment," *IEEE Trans. Antennas Propagat.*, vol. 39, pp. 1575–1586, Nov. 1991.
- [3] Y. Guo, K. Lee, P. A. Stimson, K. Potter, and D. B. Rutledge, "Aperture efficiency of integrated-circuit horn antennas," *Microwave Optical Tech. Lett.*, vol. 4, no. 1, pp. 6–9, Jan. 1991.
- [4] W. Y. Ali-Ahmad and G. M. Rebeiz, "92 GHz dual-polarized integrated horn antennas," *IEEE Trans. Antennas Propagat.*, vol. 39, July 1991.
- [5] A. W. Love, "The diagonal horn antenna," *Microwave J.*, vol. V, pp. 117–122, Mar. 1962.
- [6] J. F. Johanson and N. D. Whyborn, "The diagonal horn as a submillimeter wave antenna," *IEEE Trans. Microwave Theory Tech.*, to be published.
- [7] S. E. Schwarz, "Efficiency of quasi-optical couplers," *Int. J. Infrared Millimeter Waves*, vol. 5, no. 12, pp. 321–325, 1984.
- [8] R. J. Wylde, "Millimeter-wave Gaussian beam-mode optics and corrugated feed-horns," *Proc. Inst. Elec. Eng.*, vol. 131, pt. H, no. 4, pp. 258–262, Aug. 1984.
- [9] J. A. Murphy, "Aperture efficiencies of large axisymmetric reflector antennas fed by conical horns," *IEEE Trans. Antennas Propagat.*, vol. AP-36, pp. 570–575, Apr. 1988.
- [10] A. C. Ludwig, "The definition of cross polarization," *IEEE Trans. Antennas Propagat.*, vol. AP-21, pp. 116–119, Jan. 1973.
- [11] D. Marcuse, *Light Transmission Optics*. New York: Van Nostrand, 1972, ch. 6.
- [12] C. A. Balanis, *Antenna Theory*. New York: Wiley, 1982, ch. 12.
- [13] M. Abramowitz and I. A. Stegun, *Handbook of Mathematical Functions*. New York: Dover, 1972, ch. 22.



George V. Eleftheriades was born in Limassol, Cyprus, in May 1963. He received the Diploma in Electrical Engineering with distinction from the National Technical University of Athens, Athens, Greece in 1988 and the M.S. degree in Electrical Engineering from the University of Michigan, Ann Arbor, in December 1989.

Currently he is working towards the Ph.D. degree at the Radiation Laboratory of the University of Michigan. His research interests include millimeter-wave antennas and circuits, Gaussian-beam techniques, phased arrays and analytical techniques in Electromagnetics.

Mr. Eleftheriades received the Best Paper Award at the 1990 International Conference on Antennas, Nice, France and the "Distinguished Achievement Award" from the Electrical Engineering Department of the University of Michigan, in February 1991.

Gabriel M. Rebeiz (S'86–M'88), for a photograph and biography, see this issue, p. 794.